

A FIELD STUDY OF SNOWPACK ABLATION AT SAGEHEN CREEK FIELD STATION

Stephen Drake¹, Holly J. Oldroyd², Anne W. Nolin³, Alex Greenwald³, Sydney Weiss³,
Keith S. Jennings^{3,4}, Mikey Johnson³, and Gavin R. Shields⁵

ABSTRACT

Preliminary results of a field experiment at Sagehen Creek Field Station, CA during the 2018/2019 winter season are presented. We deployed five flux towers across a subalpine forest/meadow transition zone to compare ablation processes of proximal sites. Differences in longwave and shortwave radiation, air temperature, and sublimation were observed between the five sites, varying with solar aspect, tree density, and other locale-specific parameters. Longwave exitance from snow had a sphere of influence less than 10 m whereas shortwave insolation had a range of influence up to an order of magnitude greater and depended on sun angle and tree height. Sublimation differences between sites were magnified as wind speed increased. Drifted snow caused by an isolated tree was not significant for this warm snow site. (KEYWORDS: snow, hydrology, forest, radiation, ablation, surface energy fluxes)

INTRODUCTION

Snow water equivalent (SWE) is the standard measure of the amount of water that a seasonal snowpack will produce during spring melt. Various methods have been developed with the goal of improving spatial and temporal resolution of SWE observations. For example, satellite remote sensing platforms can be used to measure snow cover extent and duration but need to be combined with models to estimate SWE. Additionally, trees present several problems for remotely sensed products by obscuring the depth of snow that lies beneath them (SNOWPEX2, 2015). High-resolution airborne lidar measurements can be used to accurately observe snow depth, but also require model results to diagnose SWE and may produce larger uncertainties in forests relative to unforested areas. The presence of trees also introduces other processes that influence snowpack deposition and evolution. These processes operate at different spatial and temporal scales that vary with many parameters such as solar aspect, air temperature, canopy density, tree species, and wind speed to name a few. The complexity of the interactions between forest topology and these different processes has eluded a methodology of obtaining accurate, remotely sensed SWE measurements in forests. The purpose of this investigation is to obtain measurements of several key processes that impact SWE distribution across a subalpine meadow/forest interface and determine their range of influence.

METHODS

We deployed five 6-m eddy-covariance flux towers at Sagehen Creek Field Station (elevation 1943 m), Figure 1. The experiment site was located 100 m west of Sagehen Creek (latitude/longitude: 39.43°/-120.24°). We placed the flux towers in a west-east orientation along the prevailing wind direction to maximize the time that subbasin-scale source air was similar for all stations. The 350 m transect spanned a forest-meadow-forest transition to capture a range of forest density, solar aspect, and zones of potential preferential snowdrift. UL-rated Romex inside conduit from a breaker panel at the main complex of buildings powered each station. We started deploying line power on October 25, 2018 and all towers were operational by January 31, 2019. Each tower was instrumented with either a Campbell Scientific Irgason or a Campbell Scientific EC150 water vapor/carbon dioxide sensor paired with a CSAT3 sonic anemometer to obtain 20 Hz measurements of wind, sonic air temperature, water vapor concentration and carbon dioxide concentration at nominal 6-m height agl. The height of the flux towers was less than half the mean height of the surrounding trees, which localizes flux footprints, especially for towers in the forest and on the downwind side of the forest edge. Eddy-covariance and bulk transfer methods were used to calculate

Paper presented Western Snow Conference 2019

¹ Stephen Drake, Department of Physics, University of Nevada, Reno, NV, 89557, stephendrake@unr.edu

² Holly J. Oldroyd, Department of Civil and Environmental Engineering, University of California, Davis, CA, 95616

³ Anne W. Nolin, Alex Greenwald, Sydney Weiss, Keith S. Jennings, Mikey Johnson, Department of Geography, University of Nevada, Reno, NV 89557

⁴ Keith S. Jennings, Desert Research Institute, Reno, NV, 89512

⁵ Gavin R. Shields, Estuary and Oceans Science Center, San Francisco State University, San Francisco, CA, 94132

water vapor fluxes. We positioned shielded Vaisala HMP-155 thermo hygrometers at 2 m and 5 m agl to obtain 1-minute averaged air temperature and humidity measurements. Kipp & Zonen CNR4 4-component radiometers at towers 1, 3 and 4 captured short and longwave radiation measurements in 1-minute time increments.



Figure 1. Overview of flux tower locations along the 350 m transect. Towers are enumerated from west to east (Image: Google Maps).

RESULTS AND DISCUSSION

Air Temperature

First, we compare the sphere of influence that shortwave radiation has for air temperature. For three clear-sky days, we plotted composites of air temperature at 2-m height agl normalized by minimum temperature (to compare morning heating rate) in Figure 2a. At sunrise, tree shading strongly influences local air temperature. As shown in the downwelling shortwave radiation plots in Figure 2b., towers 1 and 4 (T1 and T4) remained shaded for several hours after sunrise and air temperature at T1, T4 and T5 in Figure 2a. was depressed relative to tower 3. Tower 2 was sunlit earliest and solar insolation on trees near T2 warmed air by $> 6\text{ }^{\circ}\text{C}$ relative to tower 3. As nearby trees warmed by insolation, air temperature increased faster than air in the open meadow. To some degree, these temperature anomalies can be attributed to solar loading of the thermo hygrometer shields. However, by 7:30AM, T3 was not shaded, yet the temperature at T2 increased relative to T3, suggesting that positive air temperature anomalies associated with tree warming represent real physical processes.

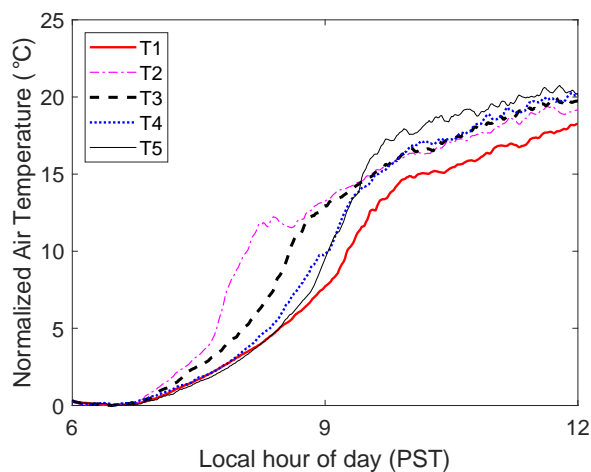


Figure 2a. 3-day composite of normalized air temperature measured at 2-m agl for each tower.

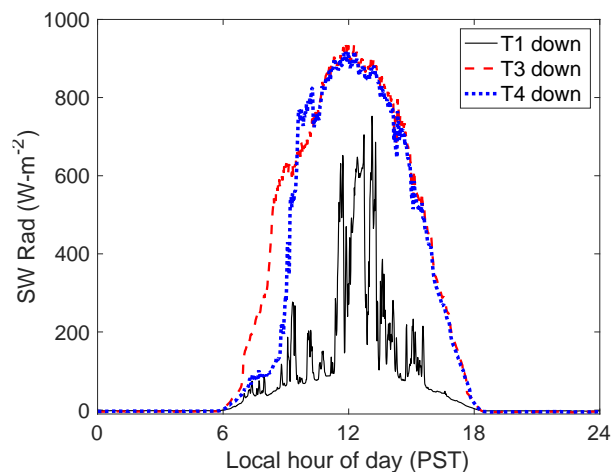


Figure 2b. 3-day composite of shortwave radiation at towers 1, 3, and 4 showing aspect-dependent solar forcing.

Periods of solar shading by large trees $> 10\text{ m}$ from tower 5 caused declines in air temperature throughout the day whereas densely-forested T1 experienced direct insolation for brief periods around midday. This analysis shows that local tree height and other canopy properties control SW radiation at a spatial scale many 10s of meters.

Surface Vapor Pressure

At towers 2 and 4 we deployed an Apogee SI-111 narrow-field infrared radiometer oriented towards the snow to measure emittance (skin temperature) of the snow surface. In Figure 3, we compare 4-day clear-sky composites of thermohygrometer-derived vapor pressure approximately 1 m above the snow surface with saturation vapor pressure derived from snow surface temperature. Assuming that air in contact with the snow surface is close to the snow surface temperature, the difference between these two measures gives the potential for sublimation and deposition at the snow surface. Figure 3 shows that saturation vapor pressure decreased below the measured vapor pressure during clear nights when the snow surface efficiently radiates, creating conditions conducive to deposition. During clear-sky days, the saturation vapor pressure increased with air temperature, creating conditions conducive to sublimation. Pomeroy et al. (2009) found that trees introduce small spatial-scale insolation variability that causes small spatial-scale variability in longwave emittance. Figure 3 supports this conclusion and additionally shows that insolation variability influences timing and spatial distribution of deposition and sublimation rates at < 10-m scale.

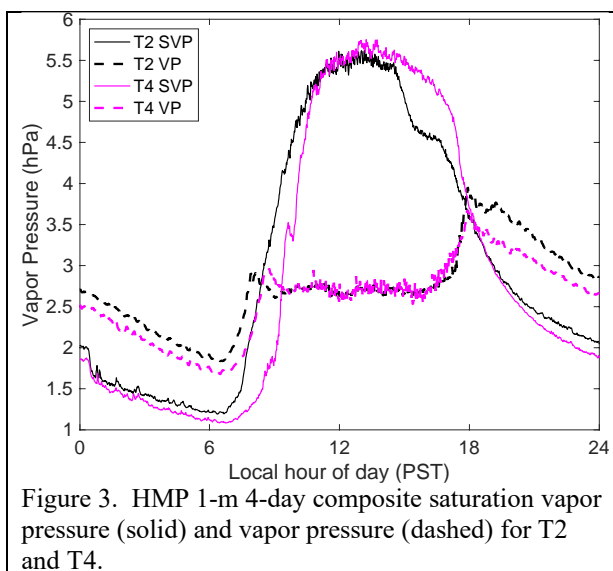


Figure 3. HMP 1-m 4-day composite saturation vapor pressure (solid) and vapor pressure (dashed) for T2 and T4.

Daily Integrated Sublimation

We present eddy-covariance derived water vapor flux measurements from two clear-sky days, April 24th and 25th, for comparison. Meteorological parameters on these two days were similar except for the average wind speed. On April 24th the average wind speed was 1.2 m·s⁻¹ and on April 25th it was 2.5 m·s⁻¹ at T3. To create Figure 4, we integrated sublimation rate for each day and divided this daily sublimation from the value found at tower 3 (in meadow). For light winds on April 24th, integrated daily sublimation was similar at all towers and slightly lower at tower 1 in dense trees. With stronger winds on April 25th, the difference in daily sublimation between towers was greater. Daily integrated sublimation was similar at towers 2, 3, and 4, which are more exposed to the wind than towers 1 and 5. The large drop in sublimation at tower 5 is an active area of investigation and is not yet fully understood. These results show that small-scale differences in sublimation rate are present across an open/forested interface and that increased wind speed enhances sublimation rate differences between open and forested areas. We note that the tree canopies were snow-free and that sublimation rates may have been higher at towers 1 and 5 had canopy-captured snow been present.

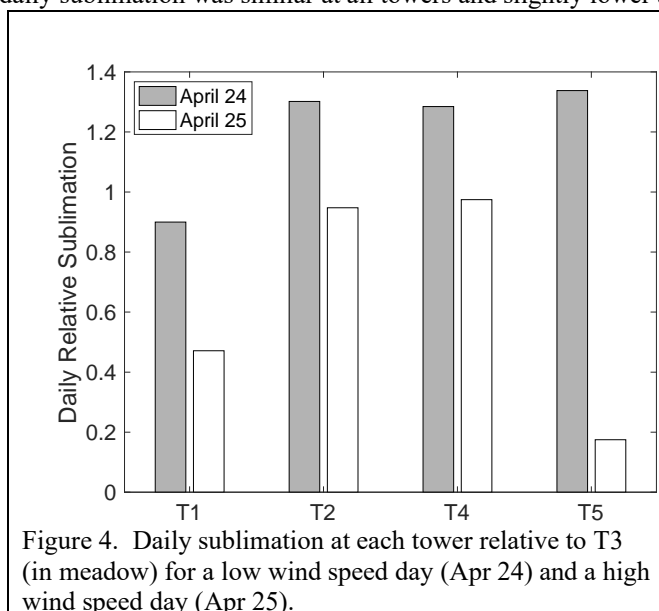


Figure 4. Daily sublimation at each tower relative to T3 (in meadow) for a low wind speed day (Apr 24) and a high wind speed day (Apr 25).

Near-Tree SWE and Snow Depths

Weekly to bi-weekly snow depth measurements acquired with a Snow Hydro Magnaprobe intervals along the tower transect revealed snow depths that varied with location and time of season. A full accounting of these results are beyond the scope of this paper. Instead, we present an anecdotal example of SWE measurements acquired radially from an isolated Lodgepole pine (*pinus murrayana*) tree on March 31, 2019 (Figure 5a.). Near-tree SWE measurements were acquired on the north side of the tree, which is downwind of the typical wind direction of approaching cold fronts. Using a Federal Sampler, we measured SWE and snow depth at 20 cm

intervals from the tree bole outward to 60 cm distance and then in 1-m intervals between 2 and 4 m from the tree bole. More distant measurements were acquired at 2-m resolution. Results are plotted in Figure 5b. with the vertical dashed line delineating the outer extent of the tree canopy. SWE depth below the tree is delineated with solid color-fill and the air space comprising the tree well space is hatch-filled. For this isolated tree, the tree well did not extend to full canopy width due to interception and subsequent throughfall. The difference in slope between the snow depth and SWE depth lines beneath the canopy indicates decreasing snow density as distance from the tree bole increases (but at a decreasing rate). At 8-m distance from the tree bole there is a slight increase in SWE that could be attributed to drifting snow, although this difference is within sampling error. If the SWE at 8m was a drift signature, this distance was the limit of the sphere of influence on drift by the tree. This anecdotal result suggests that for a warm snow site, the sphere of influence of trees on drifting snow is much smaller than for a windy, cold snow site such as studied by Marsiliano & Webb (2019). This work was performed at the University of California Natural Reserve System (Sagehen Creek Field Station), DOI: 10.21973/N33M26.



Figure 5a. SWE and tree well depth for an isolated tree were measured along the dashed line and plotted in Figure 5b.

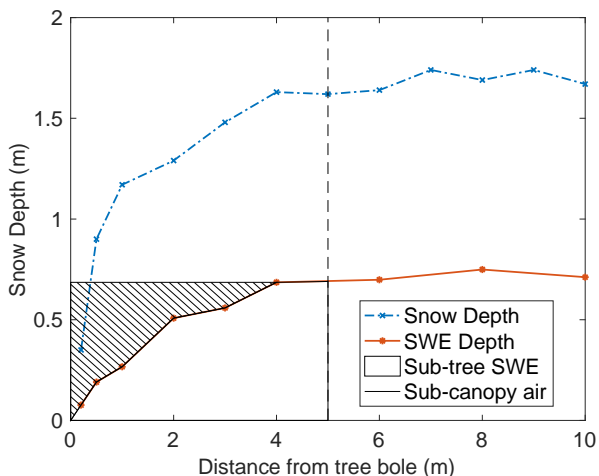


Figure 5b. Measurements of snow depth, SWE as a function of distance from the tree bole. The dashed line delineates the distance from the tree bole to the outer edge of the canopy.

CONCLUSIONS

Results of this investigation indicate that the presence of trees introduce changes in air temperature, shortwave radiation, longwave radiation, sublimation and deposition that have varying spheres of influence that, in turn, depend on forest structure. At local scale, these processes are not directly measurable by remote sensing platforms so they must be simulated with physical models to fill-in data gaps in remotely sensed products. Since these physical snowpack models are informed by field measurements, more field measurements, analysis, and comparison between sites having differing climatology are needed if we are to accurately simulate subcanopy SWE evolution.

REFERENCES

Marziliano, A. and Webb, R. 2019. Within-Stand Boundary Effects of Snow Water Equivalence Distribution in Forested Areas. *Western Snow Conference*, Reno (in Press).

Pomeroy, J. W., Marks, D., Link, T., Ellis, C., Hardy, J., Rowlands, A., & Granger, R. 2009. The impact of coniferous forest temperature on incoming longwave radiation to melting snow. *Hydrological Processes: An International Journal*, 23(17), 2513-2525.

SNOWPEX2 Workshop, September 15, 2015, Boulder, Colorado.